REVIEWS

Journal of Semiconductors
(2019) 40, 071901
doi: 10.1088/1674-4926/40/7/071901

Telecom wavelength single photon sources

Xin Cao, Michael Zopf, and Fei Ding†

Institute for Solid State Physics, Leibniz University of Hannover, Appelstraße 2, 30167 Hannover, Germany

Abstract: Single photon sources are key components for quantum technologies such as quantum communication, computing and metrology. A key challenge towards the realization of global quantum networks are transmission losses in optical fibers. Therefore, single photon sources are required to emit at the low-loss telecom wavelength bands. However, an ideal telecom wavelength single photon source has yet to be discovered. Here, we review the recent progress in realizing such sources. We start with single photon emission based on atomic ensembles and spontaneous parametric down conversion, and then focus on solid-state emitters including semiconductor quantum dots, defects in silicon carbide and carbon nanotubes. In conclusion, some state-of-the-art applications are highlighted.

Key words: telecom wavelength; single photon sources; quantum communication

Citation: X Cao, M Zopf, and F Ding, Telecom wavelength single photon sources[J]. *J. Semicond.*, 2019, 40(7), 071901. http://doi.org/10.1088/1674-4926/40/7/071901

1. Introduction

With the development of quantum computing[1, 2], current algorithms for ensuring secrecy in data communication would pose a high security risk. The most promising approach to truly secure communication is quantum communication, offering secrecy based on physical laws. Currently developed quantum cryptography systems such as quantum key distribution (QKD)[3] rely on the no-cloning theorem of quantum bits (qubit). A very famous proposal of QKD was proposed by Bennett and Brassard in 1984 (BB84)[4], using the polarization states of single photons to distribute a secret key. The presence of an eavesdropper can be easily detected due to increased error rates in the key distribution. However, there are many challenges to realize such protocols, e.g. the development of perfect single-photon sources. These are not only critical for quantum cryptography, but also for quantum computing[5], quantum metrology[6] and quantum networks[7].

The first single-photon source was created by using an emission cascade in mercury atoms[8]. Today, after more than four decades' development, there are many different types of single-photon sources, such as atomic ensembles[9], ion traps[10], single molecules[11, 12], semiconductor quantum dots (QDs)[13], defects in diamonds[14, 15], non-linear crystals[16], and many more[17]. With these sources, several QKD experiments have been realized in free-space, from laboratory scale of tens of centimetres to over 10 km[18–20]. The wavelength used in these experiments ranged from 550 to 780 nm. However, increasing the QKD distance using that wavelength range is very challenging due to low signal-to-noise ratios: On one hand, solar radiation strongly contributes to the background, since it is relatively high at that wavelength range (Fig. 1(a)). On the other hand, Rayleigh scattering in the atmosphere is proportional to $1/\lambda^4$ and therefore adds to the noise for short wavelength. In addition, practical applications vastly require data transmission over optical fibers. Due to the signal attenuation in the fiber, the loss of photons within visible wavelength range is more than 3 dB/km (see Fig. 1(b)), which is unsuitable for long-distance transmission. The two telecommunication windows with minimized attenuation at 1310 and 1550 nm, which are known as the O-band (0.3 dB/km) and C-band (0.15 dB/km), are more applicable and are widely used in the fiber-based long-distance telecommunications. Because of the relatively low solar radiation and Rayleigh scattering at these two windows, they are also applicable to free-space telecommunication. Therefore, many efforts are now spent on producing single-photon source at telecom wavelength.

Correspondence to: F Ding, f.ding@fkp.uni-hannover.de
Received 7 MAY 2019; Revised 5 JUNE 2019.

2. Single photon emission

2.1. Concept

An ideal single-photon emission consists of exactly one photon at a time, which can be triggered on-demand, meaning that the user can emit a single photon at will. Furthermore, the emitted photons should be indistinguishable[23]. A simple two-level scheme of single-photon emission is shown in Fig. 2. One electron is excited to an excited state (high level) by an external pulse, then within a certain time it falls back to the ground state (low level) emitting a single photon.

The single photon emission should obey sub-Poissonian statistics:

$$\Delta n < \sqrt{\bar{n}}, \tag{1}$$

where Δn is the standard deviation of the photon numbers in a certain time interval, and $\bar{n}$ is the average number of photons.

However, it is experimentally challenging to meet these properties. Often, there is only a certain probability to get single photon per trigger. In many cases, we get no photon or multi-photons. Therefore, the emission properties need to be precisely characterized with regard to the single-photon character.

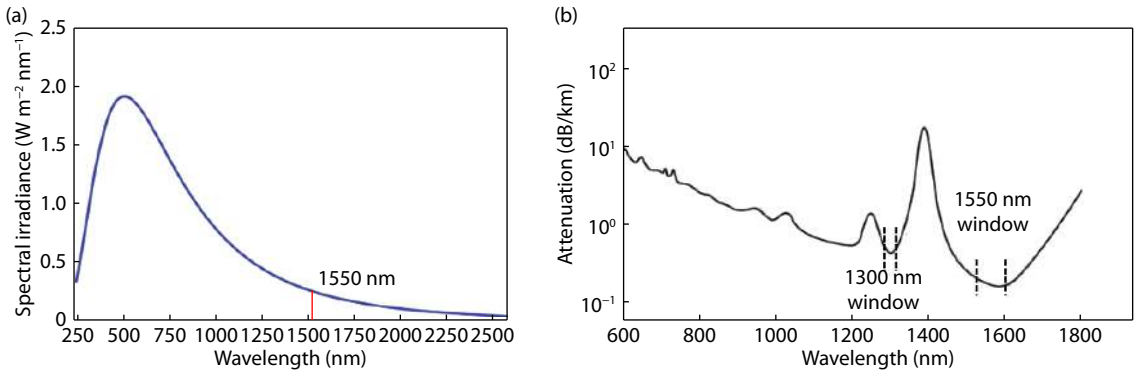

Fig. 1. (Color online) (a) Solar radiation spectrum from UV to near-infrared light. (b) Photon attenuation in optical fiber as a function of wavelength. Wavelengths at 1300 and 1550 nm are called telecom O-band and C-band, respectively, which are commonly used in fiber-based applications. (a) Adapted with permission from Ref. [21]. (Springer Nature) (b) Adapted from Ref. [22].

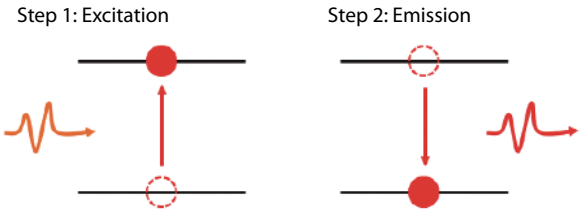

Fig. 2. (Color online) Scheme of single photon excitation and emission in a two-level system.

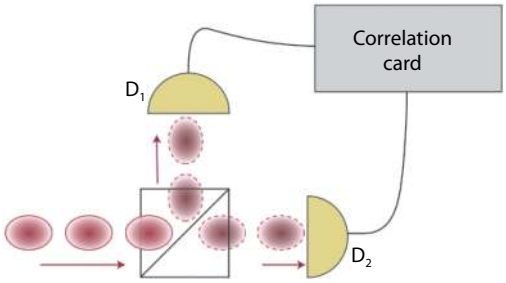

Fig. 3. (Color online) Scheme of Hanbury Brown and Twiss setup for autocorrelation measurement. The beam of light is sent to a beam splitter with single-photon detectors at the two outputs. An electronic correlator then determines the time delay between the two detector signals. Single photon emission results in the absence of simultaneous detection events on D_1 and D_2, in contrast to the case of multi-photon emission. Reprinted with permission from Ref. [24]. (Springer Nature)

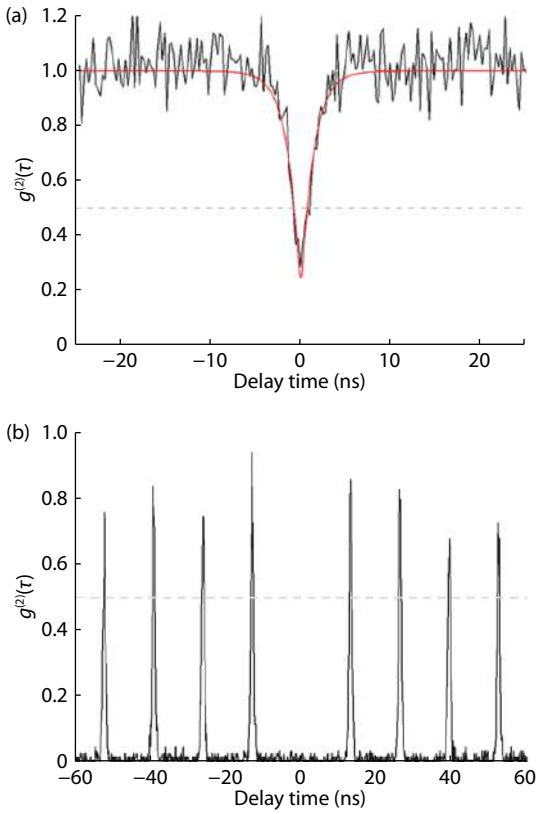

Fig. 4. (Color online) Second order correlation function measured under two types of optical excitations. (a) Continuous wave excitation. (b) Pulsed excitation.

2.2. Characterization of single-photon emission

In order to measure whether the light source emits single or multiple photons, the Hanbury Brown and Twiss experiment may be performed[25]. The setup is shown in Fig. 3. The photons are sent to a non-polarizing 50 : 50 beam splitter. Two single-photon detectors (D_1 and D_2) are placed at the two outputs of the beam splitter and measure the photons from each output. The two detectors are connected to a correlation device which determines the time delay between the detection events. The recorded data can be displayed in a histogram, showing the second-order correlation function of the single-photon emission:

$$g^{(2)}(\tau) = \frac{\langle n_1(t) n_2(t+\tau)\rangle_t}{\langle n_1(t)\rangle_t \langle n_2(t+\tau)\rangle_t}, \quad (2)$$

where $n_i(t)$ is the photon number detected by the detector D_i at time t, and $i = 1, 2$. If the light source only emits single photons, no coincidence counts should be detected at zero time delay ($\tau = 0$). However, an imperfect source will result in the detection of photon coincidence at zero delay, as shown in Fig. 4. If $g^{(2)}(0)$ is below the classical limit of 0.5 it can be considered a single photon source.

3. Telecom wavelength single-photon sources

Compared with single photon sources emitting at the visible wavelength range, few research has been conducted on telecom sources till now. But due to their potentials in application, telecom wavelength single-photon sources are becoming more and more attractive. Table 1 lists different types of

Table 1. Summary of six types of single photon sources emitting at telecom wavelength.

Material system	Operating temperature	$g^{(2)}(0)$	Ref.
Atomic sources	Room temperature	0.06	[26]
Parametric down conversion	Room temperature	0.001 ± 0.0003	[27]
InAs quantum dots	Cryogenic temperature	0.00044 ± 0.00002	[28]
Silicon Carbide	Room temperature	0.05 ± 0.03	[29]
Carbon nanotubes	Room temperature	0.01	[30]
Gallium Nitride	Room temperature	0.05 ± 0.02	[31]

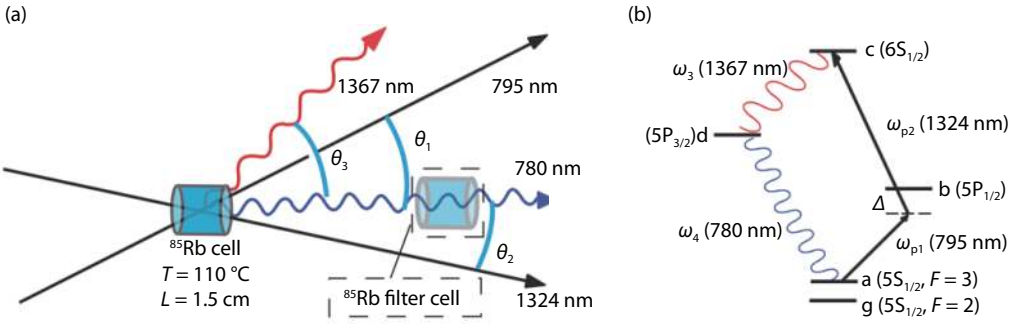

Fig. 5. (Color online) (a) Scheme of single photon emission from Rb atoms. Two pumping lasers are needed for Rb excitation (795 and 1324 nm), and two wavelength of single photons will be emitted (780 and 1367 nm). (b) The configuration of Rb energy levels. Reprinted with permission from Ref. [26]. (The Optical Society)

such single photon sources.

3.1. Atomic sources

Atomic cascade transitions were the first experimentally realized single photon sources[8]. According to quantum mechanics, single atoms have many discrete energy levels. The transition between each two levels correspond to a certain energy (or photon wavelength, from ultraviolet to infrared range). Many of these transitions emit photons in the visible wavelength range[32–34]. However, in the last decade a lot of efforts were put on erbium ions[35], atomic rubidium, cesium, sodium, potassium as well as atomic ensembles[36]. The erbium ion $^4I_{13/2}$ to $^4I_{15/2}$ transition can emit photon with wavelength at 1.5 μm while rubidium and caesium atomic transitions can span the whole telecom O-band and C-band.

By using two lasers to pump the hot rubidium vapour cell, a cascade transition will occur and two single photons will be generated, one with short wavelength at 780 nm and the other within the telecom O-band[26, 37] (Fig. 5). After filtering one wavelength, single photon emission at either the telecom or visible region can be obtained. Since the two photons are emitted one after another, one of the photons can act as a heralding signal for the other single photon emission. With such a cascade transition, the polarization state of the first emitted photon is correlated with the second photon polarization such that it results in polarization entanglement[26]. Determining the polarization state of one photon will simultaneously fix the second photon's polarization, which Einstein referred as 'a spooky action at a distance'. In addition, thanks to the long storage lifetime (milliseconds) of atomic ensembles[38], it is also a very good candidate for quantum memory application[39–41]. However, their low radiative rates restrict the brightness, and the limited trapping time could induce decoherence[42]. The required optical setups for trapping atoms in cavities limit the scalability of these type of single photon sources.

3.2. Spontaneous parametric down conversion

Till now, the most widely studied and used single-photon emitters are based on spontaneous parametric down conversion (SPDC). It was first experimentally achieved in 1970[43, 44]. By guiding a strong pump laser light on a second-order nonlinear crystal, e.g. β-barium borate (BBO) or a periodically poled lithium niobate (PPLN) waveguide, with a certain probability, we can obtain two beams of light with lower energy, called signal and idler[45–47]. The signal and idler photons should meet the phase matching requirement: $\omega_p = \omega_s + \omega_i$, $\boldsymbol{q}_p = \boldsymbol{q}_s + \boldsymbol{q}_i$, where ω is the frequency, $\boldsymbol{q}$ is the momentum, and p, s, i denote pump, signal, and idler photons, respectively, as shown in Fig. 6. By choosing the appropriate pump laser and nonlinear crystal, we can tune the wavelength of the emitted photons from visible range to the whole telecom band[48–53]. The down-converted photons from SPDC can easily reach indistinguishability of over 90%[54–58]. By further spectral filtering of the down-converted photons, photons with nearly unity indistinguishability can be obtained[59]. Another advantage of SPDC sources over other solid-state single-photon emitters is that it is operated at room temperature. Similar with atomic cascade transitions, one of the down-converted photons heralds the generation of the other single photon. All these properties make it a very promising single photon source for quantum information processing applications.

However, SPDC is not an 'on-demand' single-photon source. After the pump laser passes the nonlinear crystal, single photon emission can only be obtained with a certain probability. For different pump powers, either multiple photons will be emitted, or no photons are generated at most of the time. Although post-selection can ensure high single-photon emission $\left(g^{(2)}(0) = 0.001 \pm 0.0003\right)$[27], the brightness is significantly decreased.

Recently, an ultra-fast single photon source at telecom wavelength has been realized[60]. The scheme is shown in Fig. 7. The wavelength of photons emitted by a pulsed telecom laser with 10 GHz repetition rate is doubled by second harmonic generation (SHG). The photons then pump the SPDC

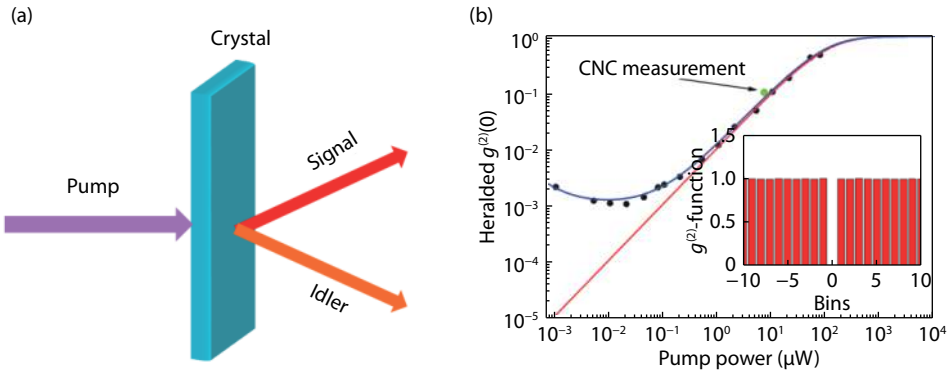

Fig. 6. (Color online) (a) Scheme of SPDC process and phase matching. (b) High purity of single photon emission. The dots are experiment data, the blue and red curves are theoretical fitting with and without considering detector noise. The inset is $g^{(2)}(0) = 0.001$. Reprinted with permission from Ref. [27]. (The Optical Society)

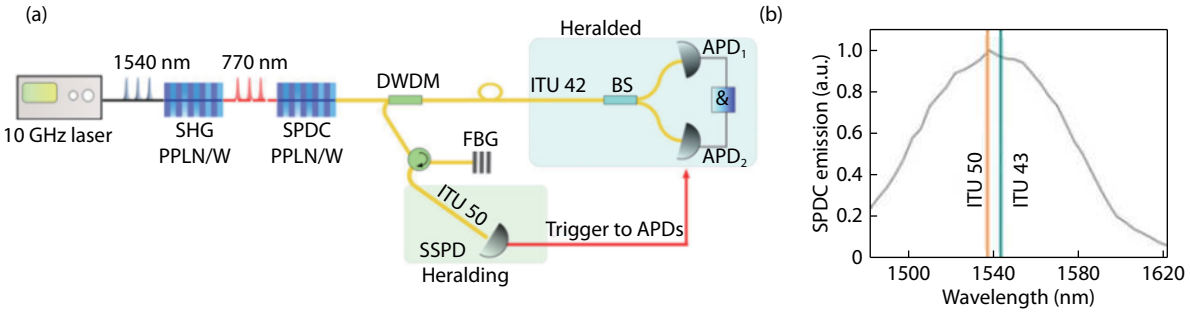

Fig. 7. (Color online) (a) Scheme of experimental setup of ultra-fast heralded single photon source. (b) Selected signal photons (ITU 50) and idler photons (ITU 43) from the SPDC spectrum (black line). Reprinted with permission from Ref. [60]. (John Wiley & Sons)

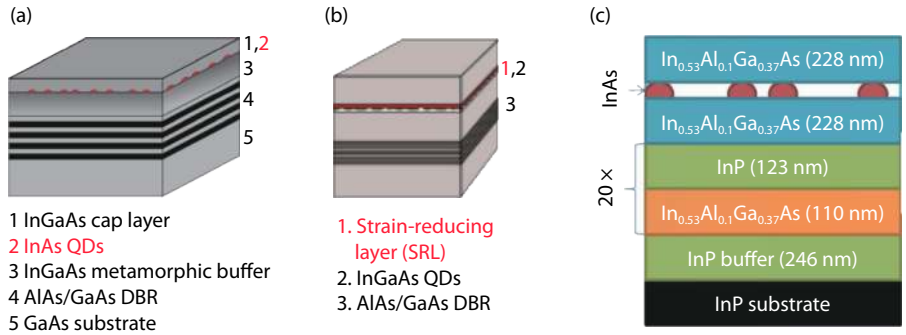

Fig. 8. (Color online) Three types of QDs grown epitaxially on GaAs and InP substrate, respectively. Reprinted with permission from Refs. [77, 81, 84]. (AIP Publishing)

non-linear crystal. Idler photons with wavelength 1543.73 nm are selected by a dense wavelength demultiplexer (DWDM) and sent to a Hanbury Brown-Twiss setup, while the signal photons with wavelength 1537.40 nm are selected by a narrow-band Bragg filter (FBG) and trigger the avalanche photodiode (APD) to herald the generation of idler photons. With the help of such ultra-fast telecom laser and non-linear optics, heralded rate of single photons at 2.1 MHz and $g^{(2)}(0)$ of 0.023 has been obtained.

3.3. Semiconductor quantum dots

Another type of well-studied single photon source is epitaxially grown semiconductor QDs. Comparing with SPDC source, QDs can achieve on-demand and therefore bright single photon emission. When a QD is excited, it will emit one single photon at a time, which is very attractive for practical applications. Furthermore, QDs can be electrically triggered[60] and are scalable due to compatibility with semiconductor technology. There are various materials systems that have been investigated so far: GaAs/GaAs[61–63], InAs/GaAs[64–67], InP/InGaP[68], InP/GaP[69, 70], InGaP/GaP[71], InGaAs/GaP[72], InGaAs/GaAs[73, 74], and more. However, due to the relatively wide band gap, almost all these material systems can only emit photons at the visible to near infrared range. Although bulk InAs has a very small band gap, the emission from InAs QDs is significantly blue-shifted[75] when grown on a GaAs substrate, due to strong strain caused by large lattice constant mismatch.

The general structure of QDs systems is shown in Fig. 8. On the substrate, the QDs layer is sandwiched between two barrier layers. The QDs have smaller band gap so that the excited electron-hole pair can be confined in the QDs. One method to

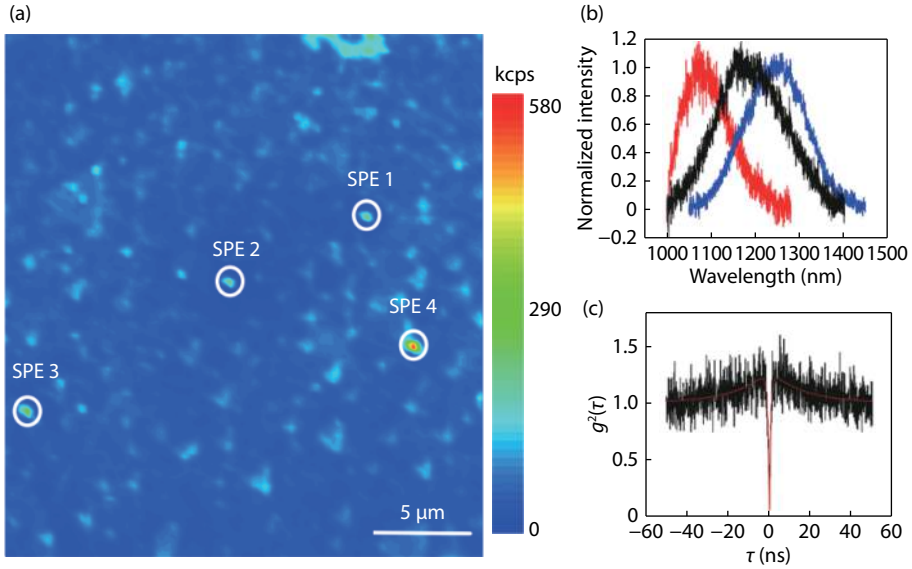

Fig. 9. (Color online) (a) Confocal map of four single photon emitters in 3C SiC epitaxy layer. (b) Room temperature photoluminescence spectra of three representative single photon emitters. (c) Second order autocorrelation measurement of the single photon emission. Reprinted with permission from Ref. [29]. (Springer Nature)

achieve telecom wavelength in the InAs/GaAs system is to grow a thick InGaAs metamorphic buffer layer between GaAs substrate and the InAs QDs[76]. With linearly increasing the In content from bottom to top, the lattice mismatch between $In_xGa_{1-x}As$ and InAs will be reduced and therefore the emission wavelength can be red-shifted to the telecom C-band[77]. The second method is to use $In_xGa_{1-x}As$ strain reducing layer[78]. After depositing the QDs, an $In_xGa_{1-x}As$ layer is used to cover the QDs instead of capping with GaAs. The lattice constant of $In_xGa_{1-x}As$ is larger than GaAs so that the strain on QDs is reduced. With the help of $In_xGa_{1-x}As$ strain reducing layers, not only InAs QDs, but also InGaAs QDs can achieve telecom wavelength emission[78–83]. The third method is to use an InP substrate. Comparing with GaAs, the lattice mismatch between InAs and InP is much smaller. Without metamorphic buffer layers or strain reducing layers, this type of InAs QDs can emit single photons at telecom C-band[28, 84–88]. However, the lattice constant of InP is much larger than silicon, making it more difficult to combine with the mature silicon technology. It is both expensive and brittle, and it is hard to grow distributed Bragg mirrors on InP wafers. Due to the small band gap of InAs as well as shallow confining potentials, the QDs can only emit single photons at very low temperature. Under cryogenic temperature and resonant pumping, very pure single photon emission with $g^{(2)}(0) = 4.4 \times 10^{-4}$ can be obtained[28]. Increasing the temperature results in a decreasing band gap of the QDs, leading to a red-shifted emission. However, more phonons will be excited at high temperature, causing photoluminescence peak broadening and degradation of the single photon emission[80]. Although we can still observe single photon emission up to 80 K, the purity is decreased significantly, with $g^{(2)}(0) = 0.34$[88].

Epitaxial QDs are usually grown by metal-organic vapour phase epitaxy or molecular beam epitaxy. The size of individual QDs is not perfectly identical, resulting in a distribution of emission wavelengths. This is detrimental for experiments requiring multiple sources of single photons, e.g. for quantum repeaters. Identical wavelengths are required to ensure the indistinguishability of photons from separate emitters. There are many ways to tune the wavelength, such as using electric field[89], magnetic field[90], strain[91–93], mainly demonstrated on non-telecom GaAs or InGaAs QDs. However, due to the difficulty to grow high quality telecom wavelength InAs QDs, very few research on wavelength tuning of InAs QDs has been reported. Till now, to the best of our knowledge, only very few group reported to use strain field to tune single photon emission at 1.55 μm with tuning range of 0.25 nm[94].

One challenge for single photon sources based on QDs is the extraction efficiency. The employed semiconductors have high refractive indices so that most of the photons are trapped in the material due to total internal reflection. Many structures are studied to enhance the extraction efficiency, such as micro-pillars[82], photonic crystals[95, 96], solid immersion lens[97], and more. However, these methods are mainly focused on GaAs-based material system emitting below 1 μm. In the case of InAs/InGaAs QDs emitting at 1.3 and 1.55 μm on InP substrate or InGaAs metamorphic buffer layer, not many fabrication techniques have been reported. Theoretically, numerical simulations showed that a cylindrical or cuboidal mesa structure with InP/AlGaInAs distributed Bragg reflector can enhance the extraction efficiency to above 25%[98]. While experimentally, extraction efficiency of 10% with InGaAs/GaAs QDs integrated into disc-shaped mesas has been reported[99]. And by using an optical horn structure, the extraction efficiency of 11% can be achieved[87]. An InAs/InP quantum dots in photonic crystal cavity can further improve the efficiency to 36%[100], which is very promising for future applications.

3.4. Defects in silicon carbide

Silicon Carbide (SiC) is a wide band gap semiconductor. There are three major polytypes: 3C-, 4H- and 6H-, with band gaps 2.36, 3.23, 3.05 eV, respectively. For studying the optical and magnetic properties, the defects in SiC are more attractive. The divacancy in 4H-SiC and carbon vacancy-antisite pair in 6H-SiC showed near infrared photon emission[101, 102], very close to the telecom wavelengths.

Recently, the single photon emission in 3C-SiC at telecom

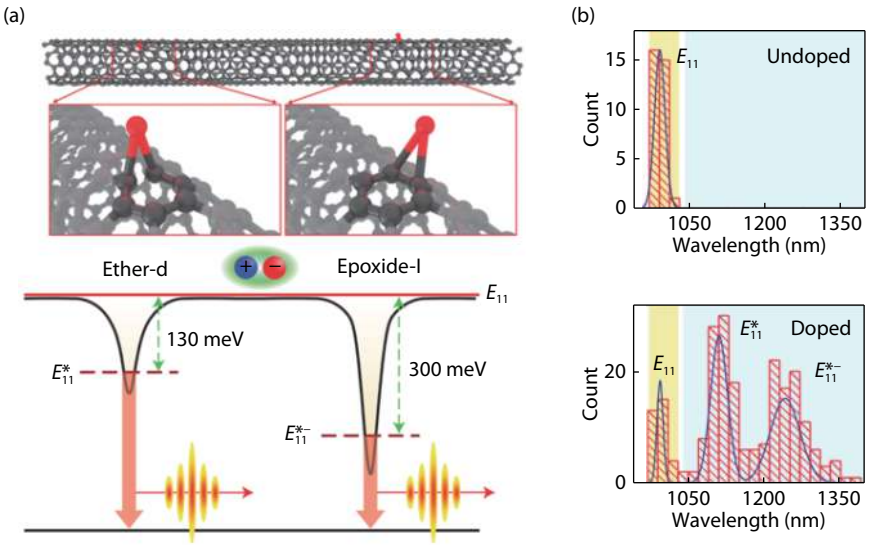

Fig. 10. (Color online) (a) Upper panel: Scheme of single wall carbon nanotube with oxygen-doping (Ether-d and Epoxide groups). Lower panel: Trap energy levels at doped areas. Oxygen-doping creates deep trap states below the E_{11} state of the nanotube, leading the localization of excitons near the doping sites. (b) Photoluminescence wavelength distribution of undoped and doped nanotubes. Reprinted with permission from Ref. [106]. (Springer Nature)

wavelength range has been reported[29]. The SiC membrane was grown epitaxially on a silicon substrate. Intrinsic defects in the 3C-SiC epitaxial layer can act as the single-photon emitters, as shown in Fig. 9. The center wavelength range of different emitters is between 1080 to 1265 nm. Such a wavelength shift (from 1080 to 1265 nm) might be caused by stacking faults in the SiC membrane. The second-order correlation function $g^{(2)}(0) = 0.05 \pm 0.03$, well below 0.5, confirms the single photon character. This telecom wavelength single-photon emitter can be operated at room temperature. Since they are grown on a silicon substrate, they can conveniently be integrated with silicon devices which is promising for future applications.

3.5. Carbon nanotubes

Carbon nanotubes have been widely studied since more than two decades ago due to their extraordinary electrical, mechanical and thermal properties[103]. After the first observation of photon antibunching in the photoluminescence measurement of a single wall carbon nanotube (SWCNT)[104], this material system became an attractive candidate for single photon sources. SWCNT is one-dimensional nanomaterial, the excitons in SWCNT are confined in two dimensions but can diffuse along the length of the nanotube[105]. To be an efficient single photon emitter, a zero-dimensional trap is required. Such a trap can be induced by the attachment of some chemical functional groups then the exciton is localized in the trap and emits single photons at cryogenic temperatures[106]. Owing to distinct lattice structures and diameters of the nanotubes, the wavelength of the single photons from undoped SWCNT can vary from around 880 to around 1140 nm[107]. With oxygen doping of the nanotubes, the wavelength can be further red-shifted to more than 1200 nm[107–109].

In addition, by introducing ether-d and eposide-I groups as the oxygen dopants to SWCNT, a deep trap state will be created below the band-edge excitons (E_{11} excitons), as shown in Fig. 10[106]. Compared to the undoped SWCNT, the wavelength of the doped SWCNT can be shifted to 1300 nm, the telecom O-band. However, the single-photon emission is relatively stable at cryogenic temperature, photoluminescence bleaching and intensity fluctuations occur when the nanotubes are placed on other solid-state substrates at higher temperatures up to room temperature[109]. In order to solve this issue, SWCNTs are encapsulated in a SiO_2 matrix on silicon so that the dopants are solitary from substrate and environment influences. With such structure, single photon emission is still possible at room temperature, with $g^{(2)}(0) = 0.32$[102]. This is also compatible with the current silicon technologies.

In order to further shift the single-photon emission to telecom C-band, the aryl sp^3 defects are introduced in carbon nanotubes[30] (Fig. 11). By choosing proper dopants, chiralities of the structure and diameters of the nanotube, the emission wavelength can span the whole telecom range. The defect states are isolated from the tails of the band-edge states and the emitter can still generate highly pure single photons, even at room temperature.

4. Applications of single photon sources

Single photon sources have many applications. The most important and practical application for telecom wavelength single photon sources is quantum key distribution thanks for the low transmission loss in optical fiber and free-space. Quantum teleportation is also an important part among quantum technologies. Till now, the main workhorse of single photon source is the SPDC source.

4.1. Quantum key distribution (QKD)

After Bennett and Brassard's proposal in 1984[4], many researches are focused on experimental realization of QKD and its distance-enhancement. Details of QKD has been reviewed in Ref. [3]. In the last few years, some big steps for commercial QKD applications have been achieved. The big challenge of free space QKD in the daytime is to collect signals from strong solar radiation. By using telecom wavelength single photon source and with the development of fiber-coupling technology and single photon detector, over 53 km QKD in daylight

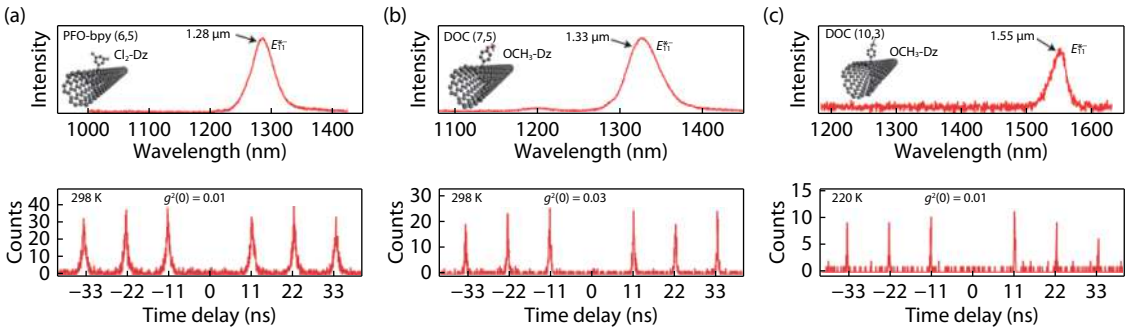

Fig. 11. (Color online) Photoluminescence spectra of two types of aryl-functionalized carbon nanotubes with different chiralities ((a) (6,5), (b) (7,5), (c) (10,3)) and their corresponding second-order correlation function. Reprinted with permission from Ref. [30]. (Springer Nature)

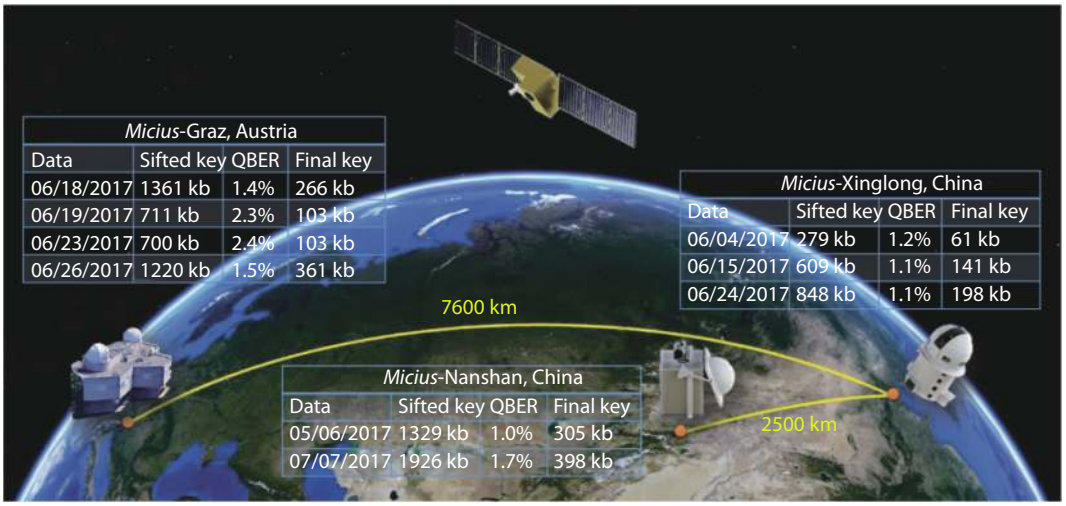

Fig. 12. (Color online) Illustration of satellite based QKD among three ground stations (Xinglong, Nanshan and Graz). Reprinted with permission from Ref. [114]. (American Physical Society)

was demonstrated with total channel loss around 48 dB[21]. Comparing with atmosphere noise, the noise in the outer space is much lower. In 2016, the quantum satellite *Micius* was launched in China, orbiting at an altitude of 500 km around earth. QKD between ground and outer space was firstly distributed over 1200 km, with a kilohertz key rate[110]. For daily applications, the most efficient way to transmit information is to use optical fibers. QKD with key rate of 1.26 Mbit/s over 50 km was implemented in 2014[111]. Two years later, the transmission distance was enhanced one order higher, to 404 km, though the key rate was decreased to 1.16 bit/h[112]. With the help of twin-field QKD scheme, QKD over 505 km with key rate about 1 bit/s was achieved[113]. However, the loss in the optical fiber channel is still very high. This may be circumvented by the implementation of proposed quantum repeaters[110]. A quantum repeater is used to restore and amplify the information that people want to send. It is an essential component for long-distance quantum computation. A practical way for long-haul QKD is to combine free space and fiber-based transmission. In 2018, an intercontinental QKD between China and Austria was illustrated (Fig. 12)[114]. The total distance was over 7600 km, which paves the way towards global quantum communication.

4.2. Quantum teleportation

Entanglement is a very important mechanism in quantum mechanics. If two photons are entangled, the state of one photon cannot be treated independently from the state of the other photon. Entangled photon pairs can be generated directly by SPDC or cascade transitions in QDs or atoms. They can also be created by performing Bell state measurements on single photons. With entangled photons and single photons, quantum teleportation has been realized.

Quantum teleportation was first experimentally verified by teleporting the polarization of one photon to another photon in the lab[115]. Quantum teleportation is another way for quantum communication. In QKD, the sender (Alice) needs to send the qubits to the receiver (Bob) for communication. However, in teleportation, Alice doesn't need to directly send the qubits to Bob. An entangled photon pair is needed and one of the photon pair will be sent to Alice, while the other will be sent to Bob. Next Alice will perform a Bell state measurement on that photon and the photon carrying the information she wants to teleport. Then by doing unitary transformation on the photon that Bob receives, Bob can reconstruct the qubit which Alice wants to send.

Quantum teleportation was first experimentally verified by teleporting the polarization of one photon to another photon in the lab[116]. While quantum teleportation is meant for long-distance communication and as an important ingredient for global quantum networks, it is necessary to increase the teleportation distance. With metropolitan optical fiber,

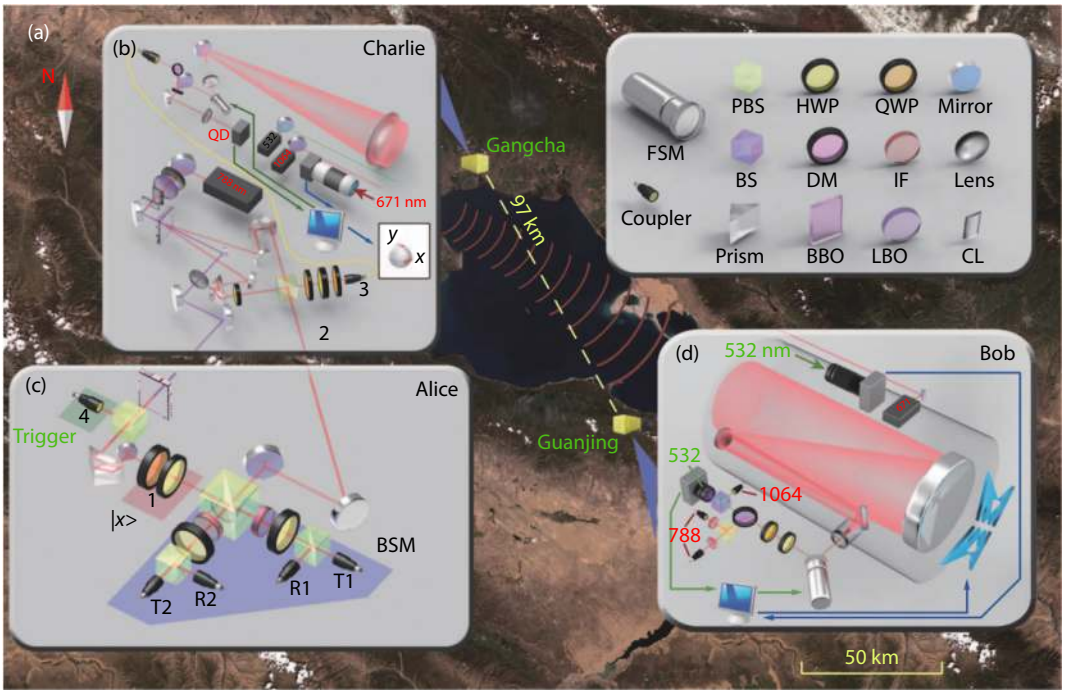

Fig. 13. (Color online) (a) Bird's-eye view of experiment site in China. (b–d) Illustration of the entangled photon pair generation and distribution from Charlie, single photon state preparation and Bell state measurement from Alice and single photon state reconstruction from Bob. Reprinted with permission from Ref. [119]. (Springer Nature)

over 10 km quantum teleportation has been achieved in the city[117, 118]. In free space, the teleportation distance can be enhanced to 100 km (Fig. 13)[119, 120]. With the launch of Micius satellite, up to 1400 km quantum teleportation has been performed, which is a crucial step towards global quantum network[121].

5. Conclusion and outlook

Single photon sources, especially at telecom wavelengths, are important constituents for quantum communication networks. Although SPDC sources have matured and are commonly used, there is a fundamental limit to its brightness. In contrast, semiconductor QDs already show great potential as bright single and entangled photon sources. Although some challenges remain to be solved, such as low extraction efficiency and relatively low photon indistinguishability, it has become the major competitor of SPDC sources. Other telecom wavelength single photon sources are being explored and yet requiring a substantial amount of research to reveal their potential for future applications.

In order to implement telecom wavelength single photon sources in real-world scenarios, electrically driven devices with small footprints are necessary. Promising QD-based photon sources have been already realized[122] which are compatible with current semiconductor technology. Another direction for quantum applications is to improve the performance of single photon sources. For experiments involving multiple sources, single photon emission with identical wavelength is required. Strain tuning and active frequency feedback are successfully applied for GaAs QDs[92, 123], and may also be useful for QDs emitting at telecom wavelength. Using resonant excitation schemes or implementing QDs in microcavities can also improve the indistinguishability of the photons[124]. Enhance the extraction efficiency of QDs equally important: Some proper methods may include integrating single photon sources into cavities or coupling with solid immersion lenses[97, 125]. To have a close-to-perfect single photon source at telecom wavelength is a milestone towards real quantum communications.

Acknowledgement

The work was financially supported by the ERC Starting Grant No. 715770 (QD-NOMS) and the National Natural Science Foundation of China (No. 61728501).

References

[1] Deutsch D. Quantum theory, the Church-Turing principle and the universal quantum computer. Proc R Soc A, 1985, 400, 97
[2] Kaltenbaek R, Walther P, Tiefenbacher F, et al. High-speed linear optics quantum computing using active feed-forward. Nature, 2007, 445, 65
[3] Scarani V, Bechmann-Pasquinucci H, Cerf N J, et al. The security of practical quantum key distribution. Rev Mod Phys, 2009, 81, 1301
[4] Bennett C H, Brassard G. Quantum cryptography: Public key distribution and coin tossing. Theor Comput Sci, 2014, 560, 7
[5] Knill E, Laflamme R, Milburn G J. A scheme for efficient quantum computation with linear optics. Nature, 2001, 409, 46
[6] Müller M, Vural H, Schneider C, et al. Quantum-dot single-photon sources for entanglement enhanced interferometry. Phys Rev Lett, 2017, 118, 257402
[7] Kimble H J. The quantum internet. Nature, 2008, 453, 1023
[8] Clauser J F. Experimental distinction between the quantum and classical field-theoretic predictions for the photoelectric effects. Phys Rev D, 1974, 9, 853
[9] Chou C W, Polyakov S V, Kuzmich A, et al. Single-photon generation from stored excitation in an atomic ensemble. Phys Rev Lett, 2004, 92, 213601
[10] Keller M, Lange B, Hayasaka K, et al. Continuous generation of single photons with controlled waveform in an ion-trap cavity

system. Nature, 2004, 431, 1075
[11] Lounis B, Moerner W E. Single photons on demand from a single molecule at room temperature. Nature, 2000, 407, 491
[12] Alléaume R, Treussart F, Courty J M, et al. Photon statistics characterization of a single-photon source. New J Phys, 2004, 6, 85
[13] Michler P, Kiraz A, Becher C, et al. A quantum dot single-photon turnstile device. Science, 2000, 290, 2282
[14] Brouri R, Beveratos A, Poizat J P, et al. Photon antibunching in the fluorescence of individual color centers in diamond. Opt Lett, 2000, 25, 1294
[15] Neu E, Steinmetz D, Riedrich-Möller J, et al. Single photon emission from silicon-vacancy colour centres in chemical vapour deposition nano-diamonds on iridium. New J Phys, 2011, 13, 025012
[16] Wang Q, Chen W, Xavier G, et al. Experimental decoy-state quantum key distribution with a sub-poissionian heralded single-photon source. Phys Rev Lett, 2008, 100, 090501
[17] Eisaman M D, Fan J, Migdall A, et al. Single-photon sources and detectors. Rev Sci Instrum, 2011, 82, 071101
[18] Bennett C H, Bessette F, Brassard G, et al. Experimental quantum cryptography. J Cryptol, 1992, 5, 3
[19] Hughes R J, Buttler W T, Kwiat P G, et al. Free-space quantum key distribution in daylight. J Mod Opt, 2000, 47, 549
[20] Hughes R J, Nordholt J E, Derkacs D, et al. Practical free-space quantum key distribution over 10 km in daylight and at night. New J Phys, 2002, 4, 343
[21] Liao S K, Yong H L, Liu C, et al. Long-distance free-space quantum key distribution in daylight towards inter-satellite communication. Nat Photonics, 2017, 11, 509
[22] Martín-Mateos P. New spectroscopic techniques and architectures for environmental and biomedical applications. PhD Dissertaion, Universidad Carlos III De Madrid, 2015
[23] Lounis B, Orrit M. Single-photon sources. Rep Prog Phys, 2005, 68, 1129
[24] Senellart P, Solomon G, White A. High-performance semiconductor quantum-dot single-photon sources. Nat Nanotechnol, 2017, 12, 1026
[25] Hanbury Brown R, Twiss R Q. Correlation between photons in two coherent beams of light. Nature, 1956, 177, 27
[26] Willis R T, Becerra F E, Orozco L A, et al. Photon statistics and polarization correlations at telecommunications wavelengths from a warm atomic ensemble. Opt Express, 2011, 19, 14632
[27] Bock M, Lenhard A, Chunnilall C, et al. Highly efficient heralded single-photon source for telecom wavelengths based on a PPLN waveguide. Opt Express, 2016, 24, 23992
[28] Miyazawa T, Takemoto K, Nambu Y, et al. Single-photon emission at 1.5 μm from an InAs / InP quantum dot with highly suppressed multi-photon emission probabilities. Appl Phys Lett, 2016, 109, 132106
[29] Wang J, Zhou Y, Wang Z, et al. Bright room temperature single photon source at telecom range in cubic silicon carbide. Nat Commun, 2018, 9, 4106
[30] He X, Hartmann N F, Ma X, et al. Tunable room-temperature single-photon emission at telecom wavelengths from sp3 defects in carbon nanotubes. Nat Photonics, 2017, 11, 577
[31] Zhou Y, Wang Z, Rasmita A, et al. Room temperature solid-state quantum emitters in the telecom range. Sci Adv, 2018, 4, eaar3580
[32] Kolesov R, Xia K, Reuter R, et al. Optical detection of a single rare-earth ion in a crystal. Nat Commun, 2012, 3, 1029
[33] Utikal T, Eichhammer E, Petersen L, et al. Spectroscopic detection and state preparation of a single praseodymium ion in a crystal. Nat Commun, 2014, 5, 3627
[34] Nakamura I, Yoshihiro T, Inagawa H, et al. Spectroscopy of single Pr^{3+} ion in LaF_3 crystal at 1.5 K. Sci Rep, 2014, 4, 7364
[35] Yin C, Rancic M, de Boo G G, et al. Optical addressing of an individual erbium ion in silicon. Nature, 213, 497, 91
[36] Chanelière T, Matsukevich D N, Jenkins S D, et al. Quantum telecommunication based on atomic cascade transitions. Phys Rev Lett, 2006, 96, 093604
[37] Jenkins S D, Matsukevich D N, Chanelière T, et al. Quantum telecommunication with atomic ensembles. J Opt Soc Am B, 2007, 24, 316
[38] Bao X, Reingruber A, Dietrich P, et al. Efficient and long-lived quantum memory with cold atoms inside a ring cavity. Nat Phys, 2012, 8, 517
[39] Saglamyurek E, Jin J, Verma V B, et al. Quantum storage of entangled telecom-wavelength photons in an erbium-doped optical fibre. Nat Photonics, 2015, 9, 83
[40] Bussières F, Clausen C, Tiranov A, et al. Quantum teleportation from a telecom-wavelength photon to a solid-state quantum memory. Nat Photonics, 2014, 8, 775
[41] Maring N, Farrera P, Kutluer K, et al. Photonic quantum state transfer between a cold atomic gas and a crystal. Nature, 2017, 551, 485
[42] Mckeever J, Boca A, Boozer A D, et al. Deterministic generation of single photons from one atom trapped in a cavity. Science, 2004, 303, 1992
[43] Klyshko D N, Penin A N, Polkovnikov B F. Parametric luminescence and light scattering by polaritons. JETP Lett, 1970, 11, 5
[44] Production P. Observation of simultaneity in parametric production of optical photon pairs. Phys Rev Lett, 1970, 25, 84
[45] Pan J W, Chen Z B, Lu C Y, et al. Multiphoton entanglement and interferometry. Rev Mod Phys, 2012, 84, 777
[46] Fujii G, Namekata N, Motoya M, et al. Bright narrowband source of photon pairs at optical telecommunication wavelengths using a type-II periodically poled lithium niobate waveguide. Opt Express, 2007, 15, 12769
[47] Xue Y, Yoshizawa A, Tsuchida H. Polarization-based entanglement swapping at the telecommunication wavelength using spontaneous parametric down-conversion photon-pair sources. Phys Rev A, 2012, 85, 032337
[48] Lo R, Jiang H, Rogers S, et al. On-chip second-harmonic generation and broadband parametric down-conversion in a lithium niobate microresonator. Opt Express, 2017, 25, 24531
[49] Jin R, Shimizu R, Wakui K, et al. Widely tunable single photon source with high purity at telecom wavelength. Opt Express, 2013, 21, 10659
[50] Zaske S, Lenhard A, Becher C. Efficient frequency downconversion at the single photon level from the red spectral range to the telecommunications C-band. Opt Express, 2011, 19, 12825
[51] Fekete J, Rieländer D, Cristiani M, et al. Ultranarrow-band photon-pair source compatible with solid state quantum memories and telecommunication networks. Phys Rev Lett, 2013, 110, 220502
[52] Zaske S, Lenhard A, Keßler C A, et al. Visible-to-telecom quantum frequency conversion of light from a single quantum emitter. Phys Rev Lett, 2012, 109, 147404
[53] Fasel S, Alibart O, Tanzilli S, et al. High-quality asynchronous heralded single-photon source at telecom wavelength High-quality asynchronous heralded single-photon source at telecom wavelength. New J Phys, 2004, 6, 163
[54] Wolfgramm F, Xing X, Cerè A, et al. Bright filter-free source of indistinguishable photon pairs. Opt Express, 2008, 16, 18145
[55] Ahlrichs A, Benson O. Bright source of indistinguishable photons based on cavity-enhanced parametric down- conversion utilizing the cluster effect parametric down-conversion utilizing the cluster effect. Appl Phys Lett, 2016, 108, 021111
[56] Xiong C, Zhang X, Liu Z, et al. Active temporal multiplexing of indistinguishable heralded single photons. Nat Commun, 2016, 7, 10853
[57] Wang X, Chen L, Li W, et al. Experimental ten-photon entangle-

ment. Phys Rev Lett, 2016, 117
[58] Meyer-Scott E, Prasannan N, Eigner C, et al. High-performance source of spectrally pure, polarization entangled photon pairs based on hybrid integrated-bulk optics. Opt Express, 2018, 26, 32475
[59] Osorio C I, Sangouard N, Thew R T. On the purity and indistinguishability of down-converted photons. J Phys B, 2013, 46, 055501
[60] Ngah L A, Alibart O, Labonté L, et al. Ultra-fast heralded single photon source based on telecom technology. Lasers Photonics Rev, 2015, 6, 1
[61] Keil R, Zopf M, Chen Y, et al. Solid-state ensemble of highly entangled photon sources at rubidium atomic transitions. Nat Commun, 2017, 8, 15501
[62] Atkinson P, Zallo E, Schmidt O G. Independent wavelength and density control of uniform GaAs/AlGaAs quantum dots grown by infilling self-assembled nanoholes. J Appl Phys, 2012, 112, 054303
[63] Huo Y H, Rastelli A, Schmidt O G. Ultra-small excitonic fine structure splitting in highly symmetric quantum dots on GaAs (001) substrate. Appl Phys Lett, 2013, 102, 152105
[64] Marzin J Y, Gérard J M, Izrael A, et al. Photoluminescence of single inas quantum dots obtained by self-organized growth on GaAs. Phys Rev Lett, 2000, 73, 716
[65] Grundmann M, Stier O, Bimberg D. InAs/GaAs pyramidal quantum dots: Strain distribution, optical phonons, and electronic structure. Phys Rev B, 1995, 52, 11969
[66] Fry P W, Itskevich I E, Mowbray D J, et al. Inverted electron-hole alignment in InAs-GaAs self-assembled quantum dots. Phys Rev Lett, 2000, 84, 733
[67] Heitz R, Kalburge A, Xie Q, et al. Excited states and energy relaxation in stacked InAs / GaAs quantum dots. Phys Rev B, 1998, 57, 9050
[68] Ugur A, Hatami F, Masselink W T, et al. Single-dot optical emission from ultralow density well-isolated InP quantum dots. Appl Phys Lett, 2008, 93, 143111
[69] Hatami F, Masselink W T, Schrottke L, et al. InP quantum dots embedded in GaP: Optical properties and carrier dynamics. Phys Rev B, 2003, 67, 085306
[70] Hatami F, Lordi V, Harris J S, et al. Red light-emitting diodes based on InP/GaP quantum dots. J Appl Phys, 2005, 97, 096106
[71] Song Y, Simmonds P J, Lee M L. Self-assembled GaP quantum dots on Self-assembled $In_{0.5}Ga_{0.5}As$ quantum dots on GaP. Appl Phys Lett, 2013, 97, 223110
[72] Nguyen Thanh T, Robert C, Cornet C, et al. Room temperature photoluminescence of high density (In, Ga)As/GaP quantum dots. Appl Phys Lett, 2011, 99, 143123
[73] Oshinowo J, Nishioka M, Ishida S, et al. Highly uniform InGaAs / GaAs quantum dots (~15 nm) by metalorganic chemical vapor deposition. Appl Phys Lett, 1994, 65, 1421
[74] Ramsay A J, Gopal A V, Gauger E M, et al. Damping of exciton rabi rotations by acoustic phonons in optically excited InGaAs/GaAs quantum dots. Phys Rev Lett, 2010, 104, 017402
[75] Heitz R, Veit M, Ledentsov N N, et al. Energy relaxation by multiphonon processes in InAs / GaAs quantum dots. Phys Rev B, 1997, 56, 10435
[76] Seravalli L, Trevisi G, Frigeri P, et al. Single quantum dot emission at telecom wavelengths from metamorphic InAs/InGaAs nanostructures grown on GaAs substrates. Appl Phys Lett, 2011, 98, 173112
[77] Paul M, Olbrich F, Höschele J, et al. Single-photon emission at 1.55 μm from MOVPE-grown InAs quantum dots on InGaAs/GaAs metamorphic buffers. Appl Phys Lett, 2017, 111, 033102
[78] Kettler J, Paul M, Olbrich F, et al. Single-photon and photon pair emission from MOVPE-grown In(Ga)As quantum dots: shifting the emission wavelength from 1.0 to 1.3 μm. Appl Phys B, 2016, 122, 48
[79] Ustinov V M, Maleev N A, Zhukov A E, et al. InAs / InGaAs quantum dot structures on GaAs substrates emitting at 1.3 μm. Appl Phys Lett, 1999, 74, 2815
[80] Olbrich F, Kettler J, Bayerbach M, et al. Temperature-dependent properties of single long-wavelength InGaAs quantum dots embedded in a strain reducing layer. J Appl Phys, 2017, 121, 184302
[81] Paul M, Kettler J, Zeuner K, et al. Metal-organic vapor-phase epitaxy-grown ultra-low density InGaAs/GaAs quantum dots exhibiting cascaded single-photon emission at 1.3 μm. Appl Phys Lett, 2015, 106, 122105
[82] Chen Z S, Ma B, Shang X J, et al. Bright single-photon source at 1.3 μm based on inas bilayer quantum dot in micropillar. Nanoscale Res Lett, 2017, 12, 2321
[83] Chen Z S, Ma B, Shang X J, He Y, et al. Telecommunication wavelength-band single-photon emission from single large InAs quantum dots nucleated on low-density seed quantum dots. Nanoscale Res Lett, 2016, 11, 1
[84] Benyoucef M, Yacob M, Reithmaier J P, et al. Telecom-wavelength (1.5 μm) single-photon emission from InP-based quantum dots. Appl Phys Lett, 2013, 103, 162101
[85] Takemoto K, Sakuma Y, Hirose S, et al. Observation of exciton transition in 1.3–1.55 μm band from single InAs/InP quantum dots in mesa structure. Jpn J Appl Phys, 2004, 43, 349
[86] Dusanowski L, Syperek M, Mrowinski P, et al. Single photon emission at 1.55 μm from charged and neutral exciton confined in a single quantum dash. Appl Phys Lett, 2014, 105
[87] Takemoto K, Takatsu M, Hirose S, et al. An optical horn structure for single- photon source using quantum dots at telecommunication wavelength. J Appl Phys, 2007, 101, 081720
[88] Dusanowski Ł, Syperek M, Misiewicz J, et al. Single-photon emission of InAs/InP quantum dashes at 1.55 μm and temperatures up to 80 K. Appl Phys Lett, 2016, 108, 163108
[89] Marcet S, Ohtani K, Ohno H. Vertical electric field tuning of the exciton fine structure splitting and photon correlation measurements of GaAs quantum dot. Appl Phys Lett, 2010, 96, 101117
[90] Bayer M, Ortner G, Stern O, et al. Fine structure of neutral and charged excitons in self-assembled In(Ga)As/(Al)GaAs quantum dots. Phys Rev B, 2002, 65, 195315
[91] Zhang J, Huo Y, Rastelli A, et al. Single photons on-demand from light-hole excitons in strain-engineered quantum dots. Nano Lett, 2015, 15, 422
[92] Chen Y, Zhang J, Zopf M, et al. Wavelength-tunable entangled photons from silicon-integrated III–V quantum dots. Nat Commun, 2016, 7, 10387
[93] Zhang Y, Chen Y, Mietschke M, et al. Monolithically integrated microelectromechanical systems for on-chip strain engineering of quantum dots. Nano Lett, 2016, 16, 5785
[94] Zeuner K D, Paul M, Lettner T, et al. A stable wavelength-tunable triggered source of single photons and cascaded photon pairs at the telecom C-band. arXiv: 1801.01518v1, 2018
[95] Balet L, Francardi M, Gerardino A, et al. Enhanced spontaneous emission rate from single InAs quantum dots in a photonic crystal nanocavity at telecom wavelengths. Appl Phys Lett, 2007, 91, 123115
[96] Birowosuto M D, Sumikura H, Matsuo S, et al. Fast Purcell-enhanced single photon source in 1,550-nm telecom band from a resonant quantum dot-cavity coupling. Sci Rep, 2012, 2, 321
[97] Chen Y, Zopf M, Keil R, et al. Highly-efficient extraction of entangled photons from quantum dots using a broadband optical antenna. Nat Commun, 2018, 9, 2994
[98] Mrowinski P, Sek G. Modelling the enhancement of spectrally broadband extraction efficiency of emission from single InAs/InP quantum dots at telecommunication wavelengths. Phys B, 2019, 562, 141

[99] Srocka N, Musia A, Schneider P I, et al. Enhanced photon-extraction efficiency from InGaAs / GaAs quantum dots in deterministic photonic structures at 1.3 μm fabricated by in-situ electron-beam lithography. AIP Adv, 2018, 8, 085205
[100] Kim J Y, Cai T, Richardson C J K, et al. Two-photon interference from a bright single-photon source at telecom wavelengths. Optica, 2016, 3, 577
[101] Son N T, Carlsson P, Hassan J ul, et al. Divacancy in 4H-SiC. Phys Rev Lett, 2006, 96, 055501
[102] Magnusson B, Janzén E. Optical Characterization of Deep Level Defects in SiC. Mater Sci Forum, 2005, 483–485, 341
[103] Lijima S. Helical microtubules of graphitic carbon. Nature, 1991, 354, 56
[104] Högele A, Galland C, Winger M, et al. Photon antibunching in the photoluminescence spectra of a single carbon nanotube. Phys Rev Lett, 2008, 100, 1217401
[105] Crochet J J, Duque J G, Werner J H, et al. Disorder limited exciton transport in colloidal single-wall carbon nanotubes. Nano Lett, 2012, 12, 5091
[106] Ma X, Hartmann N F, Baldwin J K S, et al. Room-temperature single-photon generation from solitary dopants of carbon nanotubes. Nat Nanotechnol, 2015, 10, 671
[107] Ghosh S, Bachilo S M, Simonette R A, et al. Oxygen doping modifies near-infrared band gaps in fluorescent single-walled carbon nanotubes. Science, 2010, 330, 1656
[108] Ma X, Baldwin J K S, Hartmann N F, et al. Solid-state approach for fabrication of photostable, oxygen-doped carbon nanotubes. Adv Funct Mater, 2015, 25, 6157
[109] Ma X, Adamska L, Yamaguchi H, et al. Electronic structure and chemical. nature, of oxygen dopant states in carbon nanotubes. ACS Nano, 2014, 8, 10782
[110] Liao S, Cai W, Liu W, et al. Satellite-to-ground quantum key distribution. Nature, 2017, 549, 43
[111] Comandar L C, Fröhlich B, Lucamarini M, et al. Room temperature single-photon detectors for high bit rate quantum key distribution. Appl Phys Lett, 2014, 104, 021101
[112] Yin H, Chen T, Yu Z, et al. Measurement-device-independent quantum key distribution over a 404 km optical fiber. Phys Rev Lett, 2016, 117, 190501
[113] Lucamarini M, Yuan Z L, Dynes J F, et al. Overcoming the rate-distance limit of quantum key distribution without quantum repeaters. Nature, 2018, 557, 400
[114] Liao S, Cai W, Handsteiner J, et al. Satellite-relayed intercontinental quantum network. Phys Rev Lett, 2018, 120, 030501
[115] Bennett C H, Brassard G, Crepeau C, et al. Teleporting an unknown quantum state via dual classical and Einstein-Podolsky-Rosen channels. Phys Rev Lett, 1993, 70, 1895
[116] Bouwmeester D, Pan J, Mattle K, et al. Experimental quantum teleportation. Nature, 1997, 390, 575
[117] Sun Q, Mao Y, Chen S, et al. Quantum teleportation with independent sources and prior entanglement distribution over a network. Nat Photonics, 2016, 10, 671
[118] Valivarthi R, Puigibert G, Zhou Q, et al. Quantum teleportation across a metropolitan fibre network. Nat Photonics, 2016, 10, 676
[119] Yin J, Ren J, Lu H, et al. Quantum teleportation and entanglement distribution over 100-kilometre free-space channels. Nature, 2012, 488, 185
[120] Ma X, Herbst T, Scheidl T, et al. Quantum teleportation over 143 kilometres using active feed-forward. Nature, 2012, 489, 269
[121] Yang M, Li L, Yang K, et al. Ground-to-satellite quantum teleportation. Nature, 2017, 549, 70
[122] Müller T, Krysa A B, Huwer J, et al. A quantum light-emitting diode for the standard telecom window around 1,550nm. Nat Commun, 2018, 9, 862
[123] Zopf M, Macha T, Keil R, et al. Frequency feedback for two-photon interference from separate quantum dots. Phys Rev B, 2018, 98, 161302
[124] Gazzano O, de Vasconcellos S M, Arnold C, et al. Bright solid-state sources of indistinguishable single photons. Nat Commun, 2013, 4, 1425
[125] Toishi M, Englund D, Faraon A, et al. High-brightness single photon source from a quantum dot in a directional-emission nanocavity. Opt Express, 2009, 17, 14618